Cancer Chemother Pharmacol (2007) 60:777–787
DOI 10.1007/s00280-007-0424-9

ORIGINAL ARTICLE

Tissue distribution and depletion kinetics of bortezomib and bortezomib-related radioactivity in male rats after single and repeated intravenous injection of ^{14}C-bortezomib

Alex Hemeryck · Rita Geerts · Johan Monbaliu · Stephan Hassler · Tom Verhaeghe · Luc Diels · Willy Verluyten · Ludy van Beijsterveldt · Rao N. V. S. Mamidi · Cor Janssen · Roland De Coster

Received: 13 October 2006 / Accepted: 15 January 2007 / Published online: 7 February 2007

Abstract
Purpose The body distribution of total radioactivity (TR) and bortezomib was investigated in male Sprague-Dawley rats after single and repeated i.v. (bolus) administration with ^{14}C-labelled bortezomib (VELCADE®) (0.2 mg/kg; 0.28 MBq./kg).
Methods Bortezomib was dosed on days 1, 4, 8, and 11 (i.e. a clinical dosing cycle) and the animals were sacrificed at selected time points following single and repeated dose administration for the quantification of TR in blood, plasma, and various tissues by liquid scintillation counting following organ dissection or by quantitative whole body autoradiography. In selected tissues, bortezomib levels were determined by LC-MS/MS.
Results In general, plasma TR levels were less than 10% of the corresponding blood concentrations. TR was rapidly and widely distributed to the tissues with only limited penetration into the central nervous system (CNS). In the tissues, highest levels of TR were measured in bortezomib-eliminating organs (liver and kidney), lymphoid tissues, and regions of rapidly dividing cells (e.g. the bone marrow, intestinal mucosa). Low TR concentrations were found in the CNS (tissue-to-blood ratio of ~0.05 after repeated dosing). With the exception of the liver, TR consisted almost exclusively of the parent drug. Tissue concentrations of TR and bortezomib increased up to about threefold from the first to the third dose administration, after which they remained constant.
Conclusion No undue tissue accumulation of TR and of bortezomib was observed in rats following a full clinical dosing cycle of bortezomib.

Keywords Bortezomib · VELCADE · Rat · Biodistribution · Repeated dosing

Abbreviations

AUC	Area under the concentration–time curve
C_{max}	Maximum concentration
CNS	Central nervous system
UD	Unchanged drug
LC-MS/MS	Liquid chromatography coupled with tandem mass spectrometry
LSC	Liquid scintillation counting
LLOQ	Lower limit of quantification
QC	Quality control
QWBA	Quantitative whole body autoradiography
T/B	Tissue-to-blood ratio
TR	Total radioactivity

Introduction

Bortezomib (VELCADE®), a dipeptide boronic acid analogue, is a potent, selective, and reversible inhibitor

A. Hemeryck (✉) · R. Geerts · J. Monbaliu · T. Verhaeghe · L. Diels · W. Verluyten · L. van Beijsterveldt · C. Janssen · R. De Coster
Global Preclinical Development, Johnson & Johnson Pharmaceutical Research & Development,
A Division of Janssen Pharmaceutica N.V., Beerse, Belgium
e-mail: ahemeryc@prdbe.jnj.com

R. N. V. S. Mamidi
Johnson & Johnson Pharmaceutical Research & Development, L.L.C., Raritan, NJ, USA

S. Hassler
Environmental Chemistry and Pharmanalytics Division, RCC Ltd, Itingen, Switzerland

of the 26S proteasome, a ubiquitous and multicatalytic enzyme that mediates many cellular regulatory signals by degrading regulatory proteins or their inhibitors. In vitro and in vivo data from animals indicate that peptidyl boronic acids are potent proteasome inhibitors, which display anti-tumour and anti-inflammatory efficacy [1]. In patients, bortezomib showed significant anti-tumour activity against a number of haematologic and non-haematologic malignancies, particularly in multiple myeloma and non-Hodgkin lymphoma [2–5]. Bortezomib is currently approved for the treatment of relapsed refractory multiple myeloma in over 75 countries worldwide including Canada, the USA, Europe, and a number of countries within Latin America and South-east Asia. Several clinical trials are ongoing, in which bortezomib is being evaluated in all stages of multiple myeloma and other solid tumour and haematological cancers ([1] available at http://www.clinicaltrials.gov/).

The tissue distribution of bortezomib-related radioactivity has previously been investigated in male Sprague-Dawley rats following a single i.v. bolus dose [6]. In this study, total radioactivity (TR) was quantified by means of quantitative whole body autoradiography (QWBA). To date, neither the tissue distribution of the parent drug (bortezomib) nor the biodistribution pattern of bortezomib- and/or drug-derived radioactivity following repeated dose administration has been studied.

The following considerations provided a rationale for conducting a repeat dose biodistribution study with bortezomib in the rat in which both unchanged drug (UD) and TR were measured.

First, mass balance data in rats and monkeys yielded incomplete recovery of administered radioactivity suggestive of extensive tissue distribution and retention of drug-derived radioactivity after a single dose with ^{14}C-labelled bortezomib [2]. The slow excretion of bortezomib-derived radioactivity may raise concerns of potential undue tissue accumulation when bortezomib is given per clinical dosing regimen (i.e. twice weekly administration for 2 weeks in a 3-week cycle) [7].

Second, recent evidence suggests that impairment of the ubiquitin-proteasome system in the central nervous system (CNS) may be implicated in various neurodegenerative diseases [8–10]. Knowledge of possible CNS penetration of bortezomib and/or metabolites is, therefore, an important aspect of the body distribution of bortezomib-derived material.

Therefore, the objectives of the present biodistribution study in the rat were to study the blood and plasma exposure and the distribution of bortezomib and of the bortezomib-related radioactivity in several tissues, including those previously identified as target organs of toxicity, after single and repeated i.v. dosing with ^{14}C-labelled bortezomib. UD levels were measured by LC-MS/MS, whereas TR levels were determined using two distinct methods: direct counting of radioactivity in dissected tissues and by QWBA. The latter technique was used to provide in situ information on distribution of drug-derived radioactivity to tissues and organs that are difficult to dissect and to investigate possible regional distributions within particular organs.

Materials and methods

Chemicals

^{14}C-bortezomib (see Fig. 1) (hydrochloride salt) synthesized by Johnson & Johnson Pharmaceutical Research & Development, L.L.C. (Spring House, PA, USA) was purified at J&JPRD (Beerse, Belgium). The purified ^{14}C-bortezomib was stored as a solution in water, with a specific activity of 5.44 MBq./mg and a radiochemical purity of 97.3%. Non-radiolabelled bortezomib (chemical purity > 99%) was supplied by Millennium Pharmaceuticals Inc. (Cambridge, MA, USA) as tri-anhydride.

Irgasafe liquid scintillation fluid was obtained from Perkin Elmer Life and Analytical Science (Boston, MA, USA). Solvable tissue solubilizer and Flo-Scint A liquid scintillation fluid were supplied by Packard Instrument Company Inc. (Meriden, CT, USA). NaCl 0.9% (Plurule®) was procured from Baxter, Lessines, Belgium. All other materials and chemicals were of analytical grade or higher.

Animals and procedures

Permission for animal studies was obtained from the local regulatory agencies, and all study protocols were

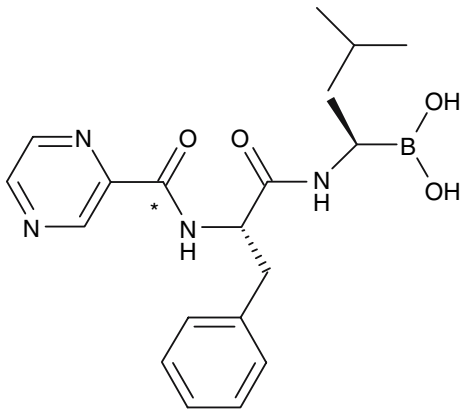

Fig. 1 Structure of ^{14}C-bortezomib. The site of labelling is indicated by an *asterisk*

in compliance with animal welfare guidelines. Thirty-three healthy male SPF Sprague-Dawley rats [CD Crtl:CD(SD)BR aged 7–8 weeks; body weight 196–244 g at dosing] were supplied by RCC Ltd Laboratory Animal Services (Füllinsdorf, Switzerland). During the pre-trial holding period, the animals were kept in groups of one to three rats under conventional hygienic conditions in Macrolone cages (Tecniplast GmbH, Hohenpeissenberg, Germany) with standard soft wood bedding. During the experiment, the animals were housed singly in open Plexiglas metabolism cages. At all times, the animals were allowed free access to water and Kliba 3433 rodent pellets (Provimi Kliba AG, Kaiseraugst, Switzerland). During the study, the animals were kept in rooms maintained at 22 ± 3°C and 40–70% relative humidity in a 12-h light/dark rhythm.

About 2 weeks prior to dosing, the dosing formulation was prepared. In brief, an appropriate amount of an aqueous solution of ^{14}C-labelled bortezomib was reduced to dryness by freeze-drying; the residue was redissolved in a sterile saline solution containing 5% (v/v) ethylalcohol. After preparation, the formulation was refrigerated until use. The final radioactivity concentration in the dosing formulation was checked by liquid scintillation counting (LSC) and found to be 561 kBq/ml. Based on this concentration of radioactivity and the specific activity, the bortezomib concentration was calculated at 0.103 mg/ml (i.e. 103% of the target concentration). The radiochemical purity of the formulation was 97.1%. At each time of dose administration, the concentration and radiochemical purity of ^{14}C-bortezomib in the formulation were verified by means of LSC and radio-HPLC. Radiolabelled bortezomib in the formulation was found to be stable since the measured ^{14}C-bortezomib levels were all within 5% of the target concentration and the radiochemical purity was >96% throughout.

The dose was administered by i.v. bolus injection at a target dose level of 0.2 mg/kg (0.28 MBq./kg) and a target dose volume of 2 ml/kg. The dose (0.2 mg/kg or 1.2 mg/m^2) is slightly below the maximum tolerated dose established in rats and it approximates the recommended clinical dose of 1.3 mg/m^2 [2]. The actual dose received by each animal was determined with reference to the dose concentration, the weight or volume of dose administered, and the specific activity of ^{14}C-bortezomib in the formulation.

The animals were sacrificed at various times post-dose for the purpose of tissue/organ excision or QWBA. On day 1 (first dose), animals (three rats per time point) were sacrificed at 10-min, 3-, 24-, and 72-h post-dose and taken for dissection. For QWBA determinations, one additional animal per time point was sacrificed at 3- and 24-h post-dose. On day 8 (third dose) at 24-h post-dose, three animals were sacrificed for organ dissection and one animal for QWBA. On day 11 (fourth dose), animals (three rats per time point) were sacrificed for organ dissection at 10-min, 3-, 24-, and 72-h post-dose. For QWBA, one additional animal was sacrificed at 3-, 24-, and 72-h post-dose.

Dissection

Animals designated for dissection were sacrificed by exsanguination following carbon dioxide anaesthesia at the specified time points following the last dose administration.

Terminal blood was collected from the thoracic cavity after heart incision and sampled into tubes containing K_3EDTA. The blood specimens were kept on melting ice pending further processing. Aliquots of at least 2 ml were separated for further analysis of TR and UD in whole blood. The remaining blood was immediately centrifuged at $1{,}500 \times g$ for 10 min in a cooled centrifuge at 4°C, plasma separated, and appropriate aliquots were separated for UD and TR analysis.

Whole blood and plasma sub samples for analysis of UD were acidified after collection prior to freezing. To each sub sample, a water/formic acid solution (50:50%, v/v) was added at a ratio of 10 µl/g sample to improve the stability of bortezomib in the biological matrix. After addition of formic acid, the sub samples were mixed on a vortex and immediately frozen at −70°C until sample analysis.

After blood sample collection, the following tissues and organs were removed from the animals by dissection and counted for TR: brain cerebellum, brain cerebrum, brain medulla, spinal cord, pituitary gland, stomach, small intestine, large intestine, diaphragm, heart, kidney, liver, lung, muscle, bone marrow, and sciatic nerve. For the purpose of UD analysis, selected tissues and organs (liver, heart, muscle, brain cerebrum, brain cerebellum, brain medulla, spinal cord, and pituitary gland) were aliquoted.

The stomach and the small and large intestines were rinsed with ice-cold saline immediately after dissection in order to remove their contents. Blood was removed from dissected tissues and organs by rinsing with ice-cold saline and blotting on filter paper.

The pituitary gland was pooled per sampling time and treatment group for analysis of UD.

To avoid drug degradation in the biological specimen, all samples were processed within 30 min following sacrifice, and the exposure to direct light was minimized.

The frozen tissue (sub) samples for UD analysis were stored at −70°C until sample analysis. The (sub) samples for TR analysis were kept frozen at −20°C until analysis.

Radioactivity measurements of excised tissues

Duplicate aliquots of plasma (0.1 ml) were mixed with 10 ml of Irgasafe scintillation fluid and subjected to LSC analysis. Aliquots of blood (0.1 ml) were first mixed with 1 ml Solvable tissue solubilizer, followed by the addition of 0.5 ml isopropanol and 0.25 ml H_2O_2 (30%). The resulting mixture was then heated to about 40°C for at least 30 min and after equilibration to room temperature, 10 ml of Irgasafe scintillation fluid was added prior to LSC.

Tissue and organ (sub) samples were manually homogenized and two aliquots of about 0.1 g each were mixed with 1 ml of Solvable tissue solubilizer. After sample digestion, the samples were equilibrated to room temperature and 10 ml of Irgasafe scintillation fluid was added prior to LSC.

All samples prepared in scintillation fluid were subjected to LSC for 10 min, together with representative blank samples, using a Liquid Scintillation Analyser (Packard 2500TR or 2900TR, Perkin Elmer, UK) with automatic quench correction. Where possible, the samples were analysed in duplicate and allowed to heat and light stabilize prior to analysis. Prior to calculation of each result, a background count rate was determined and subtracted from each sample count rate. Depending on the tissue, a lower limit of quantification (LLOQ) of 0.7–0.17 ng-eq./g was attained.

Quantitative whole body autoradiography

Animals designated for QWBA were sacrificed by a carbon dioxide overdose. After sacrifice, the hair was clipped, and the carcass was deep-frozen at approximately −80°C by immersion in a *n*-hexane/dry-ice mixture. The tail and limbs of the carcass were trimmed off, and an aqueous 4% gelatin solution was poured over the carcass. The framed specimen stage was submerged for about 30–60 min into the mixture of solid carbon dioxide and hexane until completely frozen. The frozen carcass, embedded in a solid block, was allowed to equilibrate for 12–24 h to the cryostat temperature (−20 to −25°C) prior to sectioning.

Forty-micrometer-thick sections were sliced using a cryostat microtome (Cryo Macrocut Leica CM 3600, Leica Instruments GmbH, Nussloch, Germany), collected onto adhesive tape, and lyophilized in the microtome. Five to six of the lyophilized sections of each animal were selected, covering the whole range of target tissues and organs. The selected sections together with a blood standard scale (1,000 to 5×10^6 dpm/g) were exposed on phosphor imaging plates in a lead shielded box during 2–5 days and thereafter scanned and visualized on a bio-image analysis system (BAS 5000, Fuji Film Co. Ltd, Tokyo, Japan). The processing of the images and the integration of the radioactive areas were performed on AIDA software (Raytest, Straubenhardt, Germany). The target tissues and organs were marked as area on the radioluminogram and the concentration of radioactivity was calculated as integral of the marked area expressed in photo-stimulated luminescence per mm^2. Based on the blood calibration curve, the concentration of radioactivity in tissues and organs was calculated in dpm/g and μg bortezomib equivalents/g tissue using the specific activity of ^{14}C-bortezomib. Depending on the tissue, the LLOQ ranged from 8 to 12 ng-eq./g.

LC-MS/MS determination of UD

The concentration of ^{14}C-labelled bortezomib in blood, plasma, and selected tissues and organs (brain cerebellum, cerebrum, medulla, spinal cord, pituitary gland, heart, liver, and muscle) was determined by LC-MS/MS.

Sample preparation was as follows: 0.1 ml aliquots of blood or plasma or 0.2 ml aliquots of homogenized tissue (one part tissue homogenized in nine parts of demineralized water) were spiked with 0.5 ng of internal standard (stable isotope labelled bortezomib containing nine ^{13}C atoms), acidified with 1 ml of a 0.1-M HCl solution, and extracted with 5 ml of methyl *tert*-butyl ether. All steps before the addition of the acid were carried out on melting ice to avoid degradation of the compound. Extracts were dried at 65°C under a gentle stream of nitrogen and subsequently dissolved in an injection solvent. The reconstituted extracts were analysed by LC-MS/MS consisting of a Shimadzu SIL HTC autosampler, an Agilent-1100 LC system, and an API-4000 tandem MS. Chromatography was performed on a 5 cm × 4.6 mm ID; 3.5 μm Waters Symmetry Shield RP18 column, operating at ambient temperature, with a ammonium acetate 0.01 M/methanol gradient (45/55 to 15/85, v/v) at a flow rate of 1 ml/min. The MS was operated in the negative turbo ionspray mode with mass transitions m/z 385.2 → m/z 324.0 and m/z 392.2 → m/z 331.0 being monitored for bortezomib and the internal standard, respectively. Plotting of chromatograms and peak area integrations were carried out by Analyst (version 1.2); the concentrations were calculated using Watson LIMS (version 6.4.0.02).

Validated methods were used to quantify the compound in plasma and whole blood. The assay for tissues

was not formally validated, but the stability of the analyte was confirmed in tissues from an animal dosed with cold compound.

All calibration standards and quality control (QC) samples were prepared from the dosing formulation (see under Sect. "Animals and procedures").

The plasma and whole blood calibration curve was spiked in blank, acidified rat plasma or blood and ranged from 0.5 to 200 ng/ml. For cerebellum, cerebrum, medulla, spinal cord, and pituitary gland homogenates, the calibration curve, with a range from 1 to 250 ng/g, was spiked in blank rat brain homogenate and QC samples in rat brain homogenate were analysed for batch acceptance. For heart, liver, and muscle homogenates, a calibration line was constructed in blank rat liver homogenate (range 5–2,000 ng/g) and QC samples in rat heart, liver, and muscle homogenate were taken along for batch acceptance.

For all matrices, the data from the QC samples were within the generally accepted limits for accuracy and precision [11].

Data analysis

Where possible, mean concentrations (±standard deviation) were calculated per sampling time for TR and UD in blood, plasma, and various tissues. Mean blood, plasma, and tissue concentration–time profiles of TR or UD were subjected to a non-compartmental analysis using WinNonlin® 4.1 (Pharsight, Mountain View, CA, USA). The following pharmacokinetic parameters were estimated: maximum concentration (C_{max}), time of maximum concentration (T_{max}), and the area under the concentration–time curve (AUC) from time 0 to 72 h post-dose ($AUC_{0–72\,h}$). To calculate the blood and plasma $AUC_{0–72\,h}$, the first two concentrations were used to back-calculate the level at time 0. For calculation of the tissue $AUC_{0–72\,h}$, the pre-dose levels were set to 0 or to the corresponding 72-h post-dose level in case of single or repeated dosing, respectively. When applicable, mean values (and standard deviation) were calculated for all estimated pharmacokinetic parameters.

Results

Blood and plasma kinetics, and tissue distribution of TR as determined by radioactivity counting of excised tissues

Figure 2 depicts mean ($n = 3$) concentration–time profiles of TR in blood, plasma, and some tissues (brain cerebrum, liver, and muscle) of male Sprague-Dawley rats following single and repeated (fourth dose) i.v. dosing with ^{14}C-bortezomib at 0.2 mg/kg according to a biweekly dosing regimen. The C_{max} and AUC of TR in blood, plasma, and tissues, together with tissue to blood (T/B) AUC ratios, are provided in Table 1.

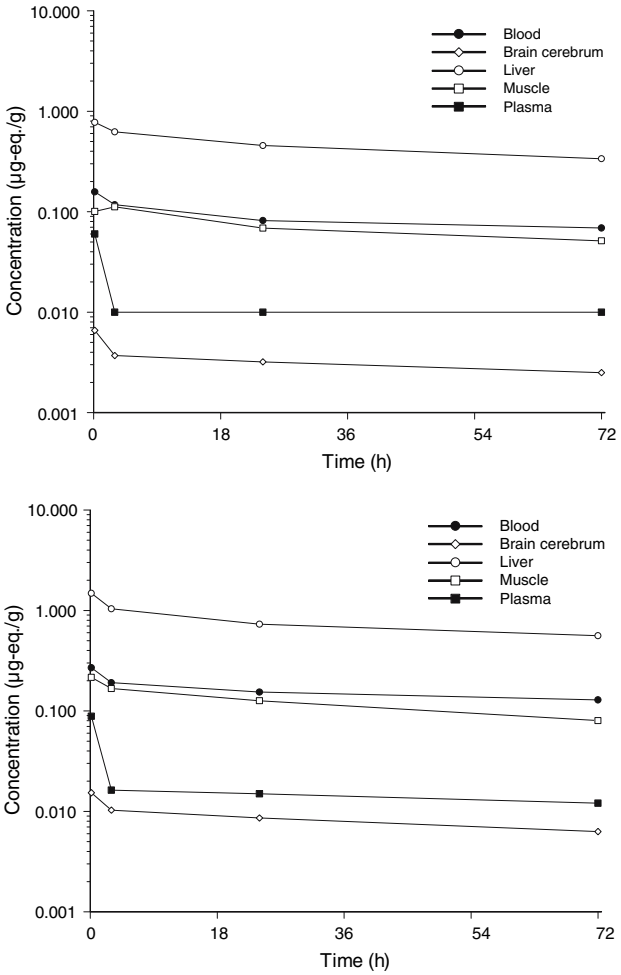

Fig. 2 Concentration–time profiles of total radioactivity in blood, plasma, and selected tissues (brain cerebrum, liver, and muscle) of male Sprague-Dawley rats after a single (*upper panel*) and repeated (fourth dose) (*lower panel*) i.v. bolus dosing with ^{14}C-bortezomib (0.2 mg/kg) according to a biweekly dosing regimen. Total radioactivity was determined by liquid scintillation counting following tissue excision

After single i.v. dosing in blood and plasma, the concentration–time profile of TR displayed an initial rapid decline up to about 3 h, followed by a more gradual decline. At 72 h after dosing, the concentration in blood and plasma had decreased to about 40 and 10% of the maximum concentrations, respectively. At C_{max}, the blood-to-plasma ratio of TR was approximately 2.5, whereas at later time points, this ratio increased up to 11–15. The exposure ($AUC_{0–72\,h}$) to TR was about 12 times higher in blood than in plasma. Taken together, these data indicate that bortezomib-related

Table 1 Mean (and SD) maximum levels (C_{max}, μg-eq./g) and areas under the concentration–time curves (AUC; μg-eq. h/g) of total radioactivity in blood, plasma, and selected tissues, together with tissue-to-blood (T/B) AUC ratios, in male Sprague-Dawley rats (n = 3/time point) after single and repeated (fourth dose) i.v. dosing with ^{14}C-bortezomib (0.2 mg/kg) according to a biweekly dosing regimen

	Single dose						Repeated dosing (fourth dose)					
	C^{a}_{max}		$AUC_{0–72\,h}$		T/B AUC ratio		C^{a}_{max}		$AUC_{0–72\,h}$		T/B AUC ratio	
	Mean	SD	Mean	SD	Mean	SD	Mean	SD	Mean	SD	Mean	SD
Blood	0.158	0.046	6.08	0.24	1.00	–	0.270	0.012	11.1	0.12	1.00	–
Plasma	0.063	0.024	0.514	0.014	0.08	0.00	0.089	0.005	1.11	0.02	0.10	0.00
Bone marrow	0.348	0.030	16.3	0.5	2.69	0.13	0.611	0.059	26.8	0.3	2.42	0.04
Brain cerebellum	0.010	0.006	0.313	0.016	0.05	0.00	0.019	0.004	0.708	0.026	0.06	0.00
Brain cerebrum	0.007	0.004	0.224	0.005	0.04	0.00	0.015	0.002	0.590	0.010	0.05	0.00
Brain medulla	0.007	0.003	0.262	0.013	0.04	0.00	0.020	0.005	0.798	0.037	0.07	0.00
Diaphragm	0.166	0.095	6.25	0.22	1.03	0.05	0.289	0.007	9.27	0.23	0.84	0.02
Heart	0.241	0.114	8.19	0.23	1.35	0.06	0.399	0.020	11.5	0.2	1.03	0.02
Kidney	0.736	0.334	22.6	0.6	3.71	0.17	1.20	0.09	33.4	0.6	3.02	0.06
Liver	0.775	0.372	32.2	0.5	5.29	0.22	1.48	0.06	52.9	1.5	4.77	0.14
Lung	0.433	0.210	15.0	0.4	2.46	0.12	0.782	0.058	22.8	0.3	2.06	0.03
Muscle	0.112	0.012	5.03	0.17	0.83	0.04	0.216	0.019	8.48	0.18	0.77	0.02
Sciatic nerve	0.086	0.013	2.18	0.07	0.36	0.02	0.086	0.007	3.47	0.07	0.31	0.01
Spinal cord	0.009	0.006	0.314	0.024	0.05	0.00	0.017	0.004	0.757	0.028	0.07	0.00
Stomach mucosa	0.243	0.138	8.66	0.29	1.42	0.07	0.411	0.016	14.0	0.2	1.26	0.03
Small intestine mucosa	0.366	0.022	13.9	0.6	2.29	0.13	0.926	0.058	21.3	0.9	1.93	0.08
Large intestine mucosa	0.259	0.019	11.4	0.4	1.88	0.09	0.411	0.037	17.1	0.4	1.54	0.04

Total radioactivity was determined by liquid scintillation counting following tissue excision

[a] Maximum levels were attained at the first sampling point (10-min post-dose), except: bone marrow, muscle, small and large intestine mucosa after single dose administration, which displayed a C_{max} at the next sampling time (3 h)

material in blood is mainly present in the corpuscular fraction.

With the notable exception of the CNS, ^{14}C-bortezomib-derived material was rapidly and widely distributed to the various tissues and organs. In general, maximum tissue TR levels were reached at the first sampling time point, i.e. 10-min (0.167 h) post-dose. Maximum levels of TR in muscle, bone marrow, and in the mucosa of small and large intestines occurred later, i.e. at the next sampling time (3-h post-dose).

The highest TR concentrations were found in the liver and kidney (three- to fivefold higher exposures than blood), followed by the lung, bone marrow, the mucosa of the gastrointestinal tract (approximately 1.4–2.7-fold higher than blood), and the diaphragm, heart, and muscle (similar to blood). TR levels in the sciatic nerve were about three times lower than in blood.

Exposure values of TR in the CNS (brain cerebrum, cerebellum and medulla, and spinal cord) were about 15–25 times lower than the corresponding blood values and amounted to maximum values of about 10 ng-eq./g.

Relative to single dose, a 1.3–2.6-fold increase in the 24-h post-dose TR levels of blood, plasma, and selected tissues was observed following the third dose administration. The 24-h-levels of TR remained fairly constant or displayed only a slight increase (up to about 1.4-fold) from the third to the fourth dose (Table 2).

The concentration–time profiles, the pattern of biodistribution, and the calculated T/B exposure ratios of TR after repeated dose administration were consistent with those observed after single dosing (Table 1; Fig. 2). After the fourth dose, the exposure ($AUC_{0–72\,h}$) in the blood, plasma, and selected tissues was 1.4–3.0-fold higher than after a single dose (Table 1).

Blood and plasma kinetics, and tissue distribution of UD after tissue excision

In Fig. 3, mean (n = 3) concentration–time profiles of bortezomib in blood, plasma, and some tissues (brain cerebrum, liver, and muscle) of male Sprague-Dawley rats following single and repeated (fourth dose) i.v. dosing with ^{14}C-bortezomib at 0.2 mg/kg according to a biweekly dosing regimen are presented. Corresponding pharmacokinetic parameters (C_{max} and $AUC_{0–72\,h}$) together with T/B and unchanged drug to total radioactivity (UD/TR) AUC ratios are provided in Table 3.

After a single i.v. dose, blood and plasma concentrations of UD resembled those of TR, indicating that TR in the systemic circulation was almost exclusively

Table 2 Mean (and SD) 24-h levels of total radioactivity (μg-eq./g) in blood, plasma, and selected tissues in male Sprague-Dawley rats ($n = 3$/time point) after single and repeated (third and fourth dose) i.v. dosing with ^{14}C-bortezomib at 0.2 mg/kg according to a biweekly dosing regimen

	First dose		Third dose		Fourth dose	
	Mean	SD	Mean	SD	Mean	SD
Blood	0.082	0.008	0.132	0.002	0.154	0.006
Plasma	0.006	0.000	0.012	0.001	0.015	0.001
Bone marrow	0.261	0.007	0.366	0.012	0.417	0.015
Brain cerebellum	0.005	0.001	0.008	0.001	0.010	0.002
Brain cerebrum	0.003	0.000	0.006	0.000	0.009	0.001
Brain medulla	0.003	0.001	0.009	0.002	0.011	0.002
Diaphragm	0.086	0.003	0.122	0.007	0.135	0.012
Heart	0.111	0.001	0.146	0.011	0.158	0.006
Kidney	0.314	0.026	0.458	0.032	0.457	0.039
Liver	0.455	0.016	0.730	0.060	0.730	0.080
Lung	0.213	0.024	0.282	0.014	0.326	0.010
Muscle	0.069	0.007	0.115	0.003	0.126	0.009
Sciatic nerve	0.030	0.002	0.055	0.005	0.052	0.002
Spinal cord	0.004	0.001	0.009	0.001	0.010	0.001
Stomach mucosa	0.117	0.005	0.189	0.008	0.201	0.002
Small intestine mucosa	0.202	0.004	0.252	0.007	0.263	0.005
Large intestine mucosa	0.185	0.001	0.241	0.003	0.245	0.020

Total radioactivity was determined by liquid scintillation counting following tissue excision

attributed to UD. With the notable exception of the liver, this was also the case in most of the examined tissues as evidenced from the UD/TR exposure ($AUC_{0–72\,h}$) ratios, which ranged from 0.63 to 0.99. In the liver, only 40% of TR was accounted for by UD.

Relative to blood, the exposure to UD was similar to three times higher in the heart, liver, and pituitary gland. In the muscle, the exposure was somewhat lower (ratio 0.66) than in blood. Similarly to TR, the exposure to UD in the CNS was markedly lower (about 20–50-fold) than in blood. The pituitary gland, which is located outside the blood-brain barrier (BBB), displayed a markedly higher exposure to UD (T/B ratio of about 3) relative to tissues that are protected by either the BBB or the blood-CSF barrier (T/B ratios of 0.02–0.04).

Compared to TR, the increase in 24-h tissue levels of UD from the first to the third dose (1.1–3.2-fold) and from the third to the fourth dose (up to 1.5-fold) was of similar magnitude (data not shown). The slightly lower 24-h concentration of UD in the pituitary gland after the third dose administration relative to the single dose is unexplained and is responsible for the somewhat higher increase in UD levels from the third to the fourth dose (about 2.3-fold).

After the fourth i.v. injection, UD concentration–time profiles, together with the calculated T/B exposure ratios, were in agreement with the single dose data

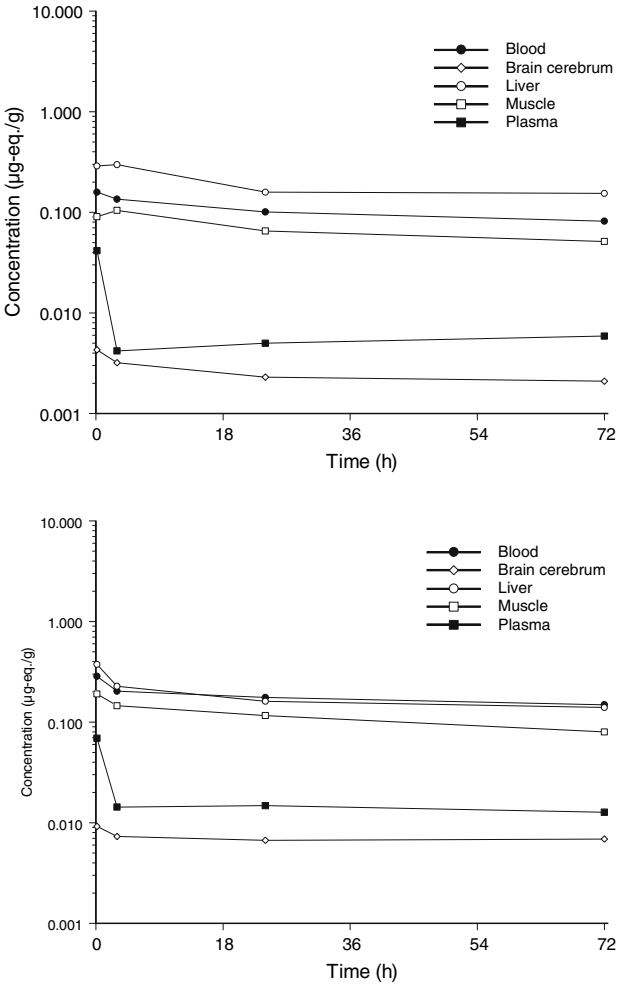

Fig. 3 Concentration–time profiles of unchanged drug (bortezomib) in blood, plasma, and selected tissues (brain cerebrum, liver, and muscle) of male Sprague-Dawley rats after a single (*upper panel*) and repeated (fourth dose) (*lower panel*) i.v. bolus dosing with ^{14}C-bortezomib (0.2 mg/kg) according to a biweekly dosing regimen. Bortezomib was measured by LC-MS/MS following tissue excision

(Table 3; Fig. 3). In line with the corresponding TR data, repeated administration with ^{14}C-bortezomib resulted in an UD exposure increase of up to 3.7-fold in blood, plasma, and selected tissues.

After repeated dosing too, UD represented the majority of the TR in the systemic circulation, as well as in the majority of the tissues investigated (Table 3). In the liver, however, UD accounted only for 23% of the radioactivity.

Tissue distribution of TR as determined by QWBA

Total radioactivity concentrations, as determined by QWBA, in the tissues after single and repeated dosing (third and fourth dose of the biweekly dosing regimen) in male Sprague-Dawley rats are listed in Table 4.

Table 3 Mean (and SD) maximum levels (C_{max}) and areas under the concentration–time curves (AUC) of bortezomib (unchanged drug, UD) in blood, plasma, and selected tissues, together with tissue to blood (T/B) and unchanged drug to total radioactivity (UD/TR) AUC ratios, in male Sprague-Dawley rats (n = 3/time point) after single and repeated (fourth dose) i.v. dosing with ^{14}C-bortezomib at 0.2 mg/kg according to a biweekly dosing regimen

	Single dose (first dose)								Repeated dosing (fourth dose)							
	C^a_{max}		$AUC_{0–72°h}$		T/B AUC ratio		UD/TR AUC ratio		C^a_{max}		$AUC_{0–72°h}$		T/B AUC ratio		UD/TR AUC ratio	
	Mean	SD	Mean	SD	Mean	SD	Mean	SD	Mean	SD	Mean	SD	Mean	SD	Mean	SD
Blood	0.159	0.038	7.27	0.27	1.00	–	1.20	0.07	0.285	0.024	12.5	0.2	1.00	–	1.13	0.02
Plasma	0.042	0.014	0.411	0.012	0.06	0.00	0.80	0.03	0.069	0.005	1.08	0.04	0.09	0.00	0.97	0.04
Brain cerebellum	0.007	0.004	0.305	0.012	0.04	0.00	0.97	0.06	0.013	0.003	0.599	0.04	0.05	0.00	0.85	0.07
Brain cerebrum	0.004	0.002	0.176	0.006	0.02	0.00	0.79	0.03	0.009	0.001	0.496	0.023	0.04	0.00	0.84	0.04
Brain medulla	0.004	0.003	0.165	0.007	0.02	0.00	0.63	0.04	0.010	0.001	0.615	0.028	0.05	0.00	0.77	0.05
Heart	0.218	0.099	8.12	0.23	1.12	0.05	0.99	0.04	0.385	0.093	10.5	0.5	0.84	0.04	0.91	0.05
Liver	0.298	0.059	13.0	2.0	1.79	0.29	0.40	0.06	0.375	0.024	12.1	0.8	0.97	0.07	0.23	0.02
Muscle	0.105	0.007	4.83	0.17	0.66	0.03	0.96	0.05	0.191	0.022	7.89	0.21	0.63	0.02	0.93	0.03
Pituitary gland	0.356	–[b]	21.5	–[b]	2.95	–[b]	n.a.[c]	–[b]	0.459	–[b]	24.7	–[b]	1.98	–[b]	n.a.[c]	–[b]
Spinal cord	0.004	0.002	0.223	0.012	0.03	0.00	0.71	0.07	0.012	0.003	0.697	0.037	0.06	0.00	0.92	0.06

Bortezomib was measured by LC-MS/MS; TR was determined by liquid scintillation counting (see Table 1)

[a] Maximum levels were attained at the first sampling point (10-min post-dose), except for the liver and muscle, which displayed a C_{max} at the next sampling occasion (3 h) after single dosing, and pituitary gland, which displayed a C_{max} at next sampling time (3 h) after single dose and at the last sampling time (24 h) after repeated dosing

[b] The pituitary gland was analysed as a pooled sample

[c] *n.a.* not available: radioactivity was not measured in the pituitary gland

Representative whole body radioluminograms from rats after the fourth i.v. dosing with ^{14}C-bortezomib at 3-, 24-, and 72-h post-dose are shown in Fig. 4.

The QWBA radioluminograms confirmed that bortezomib-related radioactivity was widely distributed to most tissues and organs with restricted distribution of drug-derived material to the CNS.

Total radioactivity concentrations determined by QWBA (Table 4) corresponded reasonably well with those determined by dissection/LSC (Table 2). The distribution pattern of radioactivity, together with the T/B ratios in tissues and organs after repeated dosing, as determined by QWBA, was comparable to that after single administration. The QWBA data confirmed that steady-state was essentially reached after three dose administrations. Moreover, QWBA provided details on tissue distribution that were not evident from the tissue excision experiments. QWBA analysis indicated that 24-h concentrations of TR in the lymph nodes were three- to fivefold higher than the corresponding blood values after single and repeated dosing. The spleen, another lymphatic organ, also demonstrated TR levels that were elevated relative to blood (five- to sevenfold at 24-h post-dose). The choroid plexus displayed a 24-h T/B ratio, which ranged from 0.36 to 0.69. Regional differences were noted in the kidney: the cortex (T/B ratios of approximately 3–4 at 24-h post-dosing) contained about twofold higher levels of radioactivity compared to the medulla. Finally, QWBA data further indicated that the concentrations of radioactivity in all areas of the CNS were either at or below the LLOQ of this technique (8–12 ng-eq./g).

Discussion

In the current study, we investigated the depletion kinetics and tissue distribution of bortezomib and its metabolites after single and repeated i.v. dosing with ^{14}C-radiolabelled bortezomib in male rats when bortezomib was given according to the clinical dosing regimen (i.e. twice weekly administration for 2 weeks in a 3-week cycle).

The concentration–time curves of TR in blood and plasma demonstrated a multiphasic profile characterized by an initial rapid distribution phase, followed by a much slower terminal phase. UD displayed a similar behaviour and represented the bulk of the radioactivity in the systemic circulation. Significantly, blood-to plasma-ratios of UD and TR were higher than unity at all time points. During the distribution phase, TR and bortezomib levels dropped more rapidly in plasma compared to blood, after which plasma levels declined in parallel to the blood levels. This resulted in markedly higher blood-to-plasma ratios in the terminal phase compared to the distribution phase. In vitro experiments confirmed the in vivo findings and provided evidence for the fact that this binding is

Table 4 Levels of total radioactivity in blood, plasma, and selected tissues in male Sprague-Dawley rats (n = 1/time point) after single and repeated i.v. dosing with ^{14}C-bortezomib (0.2 mg/kg) according to a biweekly dosing regimen

Dose	First dose		Third dose	Fourth dose		
Time post last dose (h)	3	24	24	3	24	72
Blood	0.129	0.078	0.158	0.227	0.158	0.117
Bone marrow	0.301	0.168	0.372	0.472	0.414	0.166
Brain cerebellum	<LLOQ[a]	<LLOQ	0.010	0.010	<LLOQ	<LLOQ
Brain cerebrum	<LLOQ	<LLOQ	<LLOQ	<LLOQ	<LLOQ	<LLOQ
Brain medulla	<LLOQ	<LLOQ	<LLOQ	<LLOQ	<LLOQ	<LLOQ
Choroid plexus	0.061	0.028	0.076	0.113	0.110	0.062
Diaphragm	0.179	0.113	0.160	0.286	0.155	0.122
Kidney cortex	0.540	0.329	0.437	0.773	0.449	0.439
Kidney medulla	0.247	0.192	0.210	0.402	0.218	0.163
Large intestines mucosa	0.288	0.224	0.329	0.621	0.370	0.185
Liver	0.406	0.338	0.647	0.821	0.693	0.496
Lung	0.237	0.144	0.259	0.386	0.274	0.216
Lymph nodes (mandibular)	0.262	0.246	0.709	0.604	0.646	0.655
Lymph nodes (mesenteric)	0.556	0.388	0.689	0.977	0.626	0.778
Muscle	0.135	0.078	0.130	0.182	0.128	0.104
Myocardium	0.215	0.112	0.171	0.279	0.167	0.113
Pituitary gland	0.199	0.189	0.398	0.475	0.378	0.244
Small intestine mucosa	0.451	0.285	0.334	0.524	0.336	0.158
Sciatic nerve	0.123	0.077	0.065	0.152	<LLOQ	<LLOQ
Spinal cord	<LLOQ	0.011	0.013	0.015	<LLOQ	<LLOQ
Spleen	0.613	0.549	0.786	0.946	0.923	0.707
Stomach mucosa (fundus)	0.301	0.176	0.271	0.571	0.272	0.177
Stomach mucosa (non-fundic)	0.118	0.092	0.186	0.156	0.127	0.153

Total radioactivity was determined by means of quantitative whole body autoradiography

[a] Lower limit of quantification (LLOQ) ranged from 8 to 12 ng-eq./g (depending on the tissue)

reversible and is mainly attributed to binding of bortezomib to the proteasome located in the cytosol of the red blood cell (data on file). Collectively, these data indicate that bortezomib and its metabolites are extensively distributed and retained in red blood cells.

After a single dose, as well as at steady-state, the tissue distribution of radioactivity was rapid and widespread. Distribution of radioactivity to the CNS was, however, restricted. Highest concentrations of TR were detected in organs implicated in bortezomib's elimination (i.e. the liver and kidney), lymphoid organs (e.g. the spleen and lymph nodes), and regions of rapidly dividing cells (e.g. the bone marrow and mucosal lining of the gastrointestinal tract).

In the systemic circulation, as well as in most of the tissues examined, drug-derived radioactivity was mainly accounted for by the parent drug. This was not the case for the liver, the primary organ implicated in bortezomib metabolism. In the liver, about three-quarter of the radioactivity was due to bortezomib metabolites after repeated dosing.

In vitro and in vivo studies have indicated that bortezomib is primarily metabolized by oxidative deboronation to one of two inactive enantiomers that are further processed and eliminated, both renally and in bile. In rats, monkeys, and humans, bortezomib is extensively metabolized and no UD was recovered from the excreta of rats and monkeys [2, 6]. In vitro data from human subcellular fractions showed that bortezomib is a substrate of several cytochrome P450 isoenzymes, of which CYP3A4 and CYP2C19 are considered to be the predominant isoforms implicated in its oxidative metabolism [12–15]. Importantly, the boronic acid group was found to be essential for inhibition of proteasome inhibition and the deboronated metabolites lack this pharmacological activity [13].

In the present study, levels of TR were determined in a number of tissues, including those previously identified as target organs in repeated dose toxicology studies in rodent (rat) and non-rodent (monkey) species. In these studies, haematopoietic, gastrointestinal, nephrotic, cardiac, and lymphoid system changes were demonstrated [2]. These toxicological findings correlated well with the present distribution data showing high levels of radioactivity in the bone marrow, mucosal lining of the gastrointestinal tract, kidney, heart, and lymph nodes. In addition, recent evidence suggests that the lung, an organ that also displays high levels of radioactivity, may also be a potential target tissue of bortezomib-induced toxicity [16].

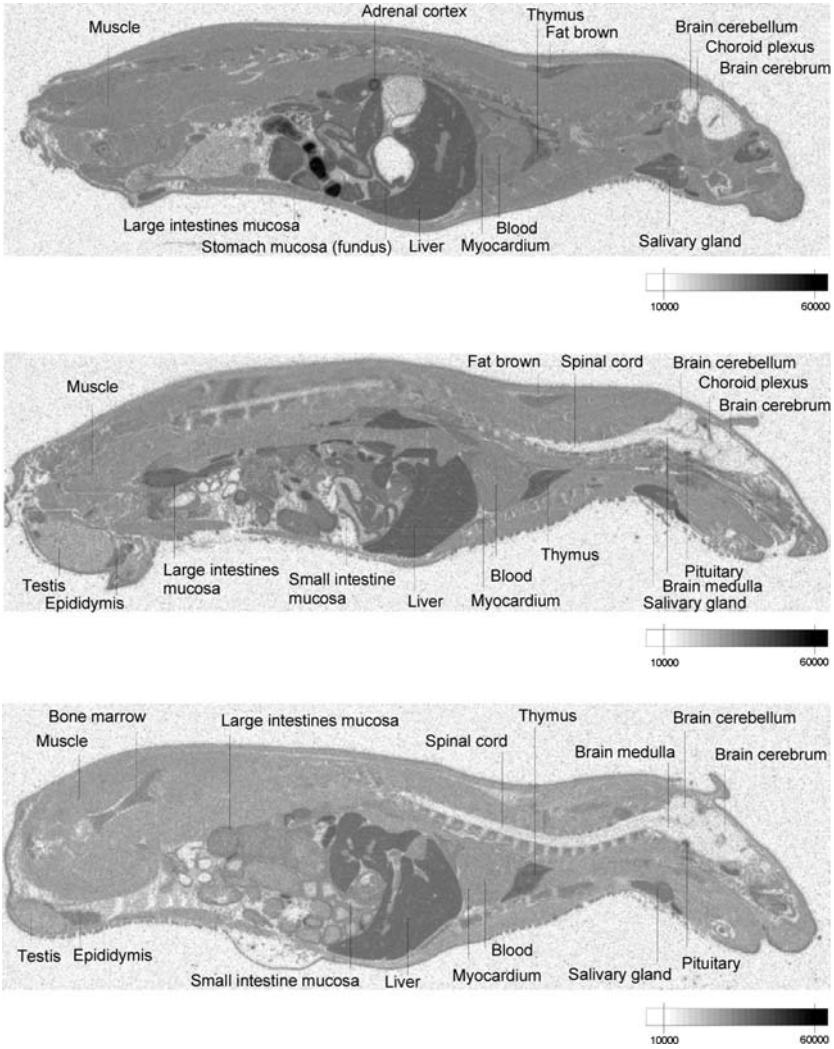

Fig. 4 Radioluminogram of male Sprague-Dawley rats at 3 h (*upper panel*), 24 h (*middle panel*), and 72 h (*lower panel*) after repeated (fourth dose) i.v. dosing with ^{14}C-bortezomib (0.2 mg/kg) according to a biweekly dosing regimen. The *bar* shows the intensity of radioactivity according to the luminogram indicator

None of the tissues showed selective accumulation, and steady-state conditions were reached from the third dose administration onwards. Importantly, bortezomib and its metabolites distributed only poorly to the tissues of the CNS. This information is of particular importance, given the growing body of evidence implicating the ubiquitin-proteasome system defects in chronic neurodegenerative diseases [9, 10]. Moreover, recent studies in rats showed that systemic exposure of rats to naturally occurring (epoxomicin) or synthetic (PSI) proteasome inhibitors induces key behavioural, pathological, and biochemical features of Parkinson's disease [8]. From a pharmacokinetic point of view, proteasome inhibitors that do not cross the BBB are preferred for clinical development.

In our study, concentrations of bortezomib and metabolites in the various brain tissues (medulla, cerebrum, and cerebellum) and the spinal cord were very low, even after repeated dose administration. As indicated by the QWBA radioluminograms, levels of radioactivity were low throughout the CNS. These data are in line with those of Adams et al. who reported that radioactivity levels in the brain and spinal cord were undetectable after a single i.v. bolus dose to Sprague-Dawley rats [6].

From the current rat study, the estimated brain-to-blood (concentration) ratio was estimated at about 0.05. However, since the employed techniques do not account for blood radioactivity present in the vascular compartment of the brain, this likely represents an overestimation. In fact, Yu et al. elegantly demonstrated that correction for blood radioactivity in the brain results in an even lower estimate of the bortezomib brain-to-blood ratio (~0.02) [17].

In the present study, it was not determined whether measured bortezomib levels in the brain were associated with significant inhibition of the proteasome in the brain. Yu et al., however, reported that bortezomib brain levels, which are twofold (C_{max} of 22 ng/g) higher than those determined in the current study; did not result in significant inhibition of proteasome activity in the brain [17]. In addition, Adams et al. reported that

efficacious doses of bortezomib, which significantly inhibit the proteasome in the blood and tumour tissue of PC-3 tumour-bearing mice, do not inhibit proteasome activity in the brain [6].

In rats, systemic drug levels of bortezomib as high as twice those attained in humans receiving the proposed therapeutic dose (1.3 mg/m^2) did not inhibit the proteasome in the brain [17], suggesting that also in the brain of VELCADE-treated patients no inhibition of the proteasome is to be expected. This is further supported by clinical safety data indicating no long-term CNS effects in VELCADE-treated subjects [4].

In conclusion, this study demonstrated that both after single and repeated i.v. administration, bortezomib and its metabolites were rapidly and extensively distributed to most tissues (including the red blood cells). Highest levels of radioactivity were measured in bortezomib-eliminating organs (the liver and kidney), lymphoid tissues, and rapidly dividing tissues (e.g. the bone marrow, intestinal mucosa). Penetration into the CNS was very limited. With the exception of the liver, measured radioactivity consisted almost exclusively of bortezomib. Finally, no undue tissue accumulation of bortezomib and its metabolites was observed in rats when bortezomib was administered according to a clinical biweekly dosing regimen.

Acknowledgments The authors would also like to express their gratitude to Willem Meuldermans (J&JPRD), Gerald Miwa, and Li Yu (Millennium Pharmaceuticals) for reviewing the manuscript. Larry Weaner and David Hoerr (J&JPRD) are acknowledged for synthesizing ^{14}C-bortezomib. Helena Geys is thanked for her contribution to the data analysis and Mia Vanthienen is acknowledged for secretarial assistance.

References

1. Montagut C, Rovira A, Mellado B, Gascon P, Ross JS, Albanell J (2005) Preclinical and clinical development of the proteasome inhibitor bortezomib in cancer treatment. Drugs Today 41(5):299–315
2. Bross PF, Kane R, Farrell AT, Abraham S, Benson K, Brower ME, Bradley S, Gobburu JV, Goheer A, Lee S-L, Leighton J, Liang CY, Lostritto RT, Guinn WD, Morse DE, Rahman A, Rosario LA, Verbois SL, Williams G, Wang Y-C, Pazdur R (2004) Approval summary for bortezomib for injection in the treatment of multiple myeloma. Clin Cancer Res 10:3954–3964
3. Ludwig H, Khayat H, Giaccone G, Facon T (2005) Proteasome inhibition and its clinical prospects in the treatment of hematologic and solid malignancies. Cancer 104:1794–1807
4. Richardson PG, Mitsiades C, Hideshima T, Anderson KC (2006) Bortezomib: proteasome inhibition as an effective anticancer therapy. Annu Rev Med 57:33–47
5. Voorhees PM, Orlowski RZ (2006) The proteasome and proteasome inhibitors in cancer therapy. Annu Rev Pharmacol Toxicol 46:189–213
6. Adams J, Palombella VJ, Sausville EA, Johnson J, Destree A, Lazarus DD, Maas J, Pien CS, Prakash S, Elliott PJ (1999) Proteasome inhibitors: a novel class of effective antitumor agents. Cancer Res 59:2615–2622
7. ICH, Committee for Medicinal Products for Human Use (CPMP) (November 1994) S3B: pharmacokinetics: guidance for repeated dose tissue distribution studies (CPMP/ICH/385/95)
8. McNaught KS, Perl DP, Brownell AL, Olanow CW (2004) Systemic exposure to proteasome inhibitors causes a progressive model of Parkinson's disease. Ann Neurol 56(1):149–162
9. Ardley HC, Hung CC, Robinson PA (2005) The aggravating role of the ubiquitin-proteasome system in neurodegeneration. FEBS Lett 579:571–576
10. Upadhya SC, Hegde AN (2005) Ubiquitin-proteasome pathway components as therapeutic maladies. Curr Pharm Des 11:3807–3828
11. FDA, U.S. Department of Health and Human Services Food and Drug Administration Center for Drug Evaluation and Research (CDER) and Center for Veterinary Medicine (CVM) (May 2001). Bioanalytical Method Validation
12. Daniels J, LaButti J, Chavan A, Huang R, Parsons I, Gan L, Miwa G (2003) Mechanistic investigations into the protein and glutathion-mediated deboronation of the peptide boronic acid proteasome inhibitors bortezomib (VELCADE™). Drug Metab Rev 35:44
13. Pekol T, Daniels JS, Labutti J, Parsons I, Nix D, Baronas E, Hsieh F, Gan LS, Miwa G (2005) Human metabolism of the proteasome inhibitor bortezomib: identification of circulating metabolites. Drug Metab Dispos 33:771–777
14. Uttamsingh V, Lu C, LaButti J, Daniels J, Huang R, Gan L, Miwa G (2003) Relative contribution of CYP isoforms to the liver microsomal intrinsic clearance of bortezomib (VELCADE™). Drug Metab Rev 35:184
15. Uttamsingh V, Lu C, Miwa G, Gan LS (2005) Relative contributions of the five major human cytochrome P450, 1A2, 2C9, 2C19, 2D6, and 3A4, to the hepatic metabolism of the proteasome inhibitor bortezomib. Drug Metab Dispos 33:1723–1728
16. Miyakoshi S, Kami M, Yuji K, Matsumura T, Takatoku M, Sasaki M, Narimatsu H, Fujii T, Kawabata M, Taniguchi S, Ozawa K, Oshimi K (2006) Severe pulmonary complications in Japanese patients after bortezomib treatment for refractory multiple myeloma. Blood 107(9):3492–3494
17. Yu LJ, Riordan B, Hatsis P, Brockman A, Daniels S, Stagliano N, Finklestein S, Ren J, Milton M, Miwa G (2006) Study of brain and whole blood PK/PD of bortezomib (VELCADE®) in rat models. J Clin Oncol. ASCO annual meeting proceedings part I, vol 24, no. 18S (June 20 Supplement):12036